mm-WAVE Op-Amps FOR LOW DISTORTION AMPLIFICATION WITH HIGH OIP3/P$_{DC}$ RATIO > 100 AT 2 GHz

Zach Griffith*, Miguel Urteaga†, and Mark J.W. Rodwell*

*Dept. of Electrical and Computer Engineering
University of California, Santa Barbara, CA 93106-9560, USA
Phone: 805-453-8011, E-mail: griffith@ece.ucsb.edu

†Teledyne Scientific and Imaging Company, 1049 Camino Dos Rios, Thousand Oaks, CA 91360, USA

***Abstract*— We here report mm-wave amplifiers employing strong global negative feedback to provide very low intermodulation distortion, using an InP DHBT technology. The amplifiers, similar to operational amplifiers, use simple- or nested-Miller compensation and have 25 to 40 GHz feedback loop bandwidths. The large loop transmission at 2 GHz provides a large reduction of closed-loop distortion at this frequency.**

A simple-compensated amplifier with 24.8 GHz bandwidth and having 1013 mW dissipation showed 13.8 dB (S$_{21}$) gain and 50.2 dBm OIP3 at (1.950, 1.975 GHz). It is unconditionally stable from DC to 15 GHz, and stable in a 50 Ω system from DC to 50 GHz. A nested-compensated amplifier with 40 GHz bandwidth and having 993 mW dissipation showed 13.8 dB (S$_{21}$) gain and 42.8 dBm OIP3 at (1.950, 1.975 GHz). It is unconditionally stable from DC-20 GHz and stable in a 50 Ω system from DC to 50 GHz. These results represent ∼ 4× increase in bandwidth for an op-amp of any kind, *as well as* ∼ 3× betterment in OIP3/P$_{DC}$ ratio at f_s = 2-3 GHz, when compared to state-of-the-art.

We address considerations important to the application of negative feedback to mm-, microwave amplifiers, including the effects of interface impedances on stability, the effect of feedback upon return losses and noise figure, and the effect of frequency compensation and of feedback topology on closed-loop distortion.

***Index Terms*— operational-amplifier, Miller compensation, intermodulation distortion**

I. INTRODUCTION

AMPLIFIERS with very low intermodulation distortion are required in radar receivers and in multi-carrier communications systems such as cell phone base stations. In simple reactively-tuned RF amplifiers the output-referred third-order intermodulation distortion intercept (OIP3) is proportional to the DC power dissipation. In this situation very low IM3 can be obtained only at the cost of high DC power consumption.

Here we report mm-wave (2 GHz) amplifiers having high (greater than 50 dBm) third-order intermodulation intercepts despite consuming a relatively low ∼ 1000 mW DC power dissipation P_{DC}. This very high ratio of third-order-intercept power to DC power consumption $P_{OIP3}/P_{DC} > 100$ is obtained through the use of strong global negative feedback using circuit techniques similar to classic operational amplifiers [1].

We explicitly distinguish this work from that of other mm-, microwave feedback amplifiers using a feedback resistor $R_f = Z_o(1 - A_v)$ [2] to provide a matched Z_o input impedance; such amplifiers have less than unity feedback magnitude. In marked contrast, low amplifier distortion is here obtained using strong global negative feedback; a mm-wave *operational amplifier*.

Obtaining high OIP3 requires novel designs and detailed attention to residual sources of distortion. Because 20-40 GHz loop bandwidths are required, stability is critically sensitive to layout and interconnect parasitics. Frequency compensation limits the degree of reduction of output-stage distortion and increases the distortion associated with stages nearer the input. Difficulties arise from inadvertent non-linear loading of the feedback network by transistor junction capacitances. Challenges include the control of input and output impedances, and the sensitivity of the loop bandwidth–i.e. phase margin to generator and load impedances. Manufacturable InP heterojunction bipolar transistor (HBT) IC technologies offer cutoff frequencies ≥ 350 GHz [3]. With appropriate design, stable feedback loops of ∼ 40 GHz bandwidth can be realized, providing strong feedback at low GHz operation for strong distortion suppression.

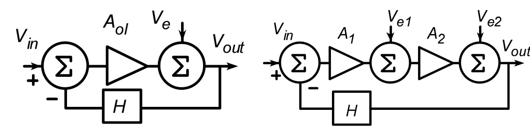

(a) (b)

Fig. 1. Error (distortion) analysis of feedback amplifiers: (a) single-stage and (b) multi-stage feedback amplifier with global feedback.

Here we report two InP DHBT based op-amps – one employing simple-Miller compensation and the other nested-Miller compensation, demonstrating 24.8 GHz and 40 GHz bandwidth respectively. The gain (S$_{21}$) is 13.8 dB and P$_{DC}$ ≅ 1000 mW. These bandwidths reflect 2.5× and 4× betterment in state-of-the-art [4] for an op-amp of any kind. Additionally, the highest OIP3(46dBm) to P$_{DC}$(1.24W) ratio (figure-of-merit) for an amplifier operating at 2-3 GHz identified by the authors is 32.2 [5]. Under two-tone operation ($f_{1,2}$ = 1.950, 1.975 GHz) the simple-Miller compensated amplifier here demonstrates very low distortion, where the OIP3 is 50.2 dBm. This corresponds to an OIP3 to P$_{DC}$ ratio of 103 – a 3.2× betterment in state-of-the-art as well.

II. THEORY

An amplifier (fig. 1a) having open-loop distortion V_e produces a closed-loop output of $V_{out} = A_{CL}V_{in} + (A_{CL}/A_{OL})V_e$, where $A_{CL} \cong 1/H$ is the closed-loop gain – distortion is reduced by the ratio (A_{CL}/A_{OL}) of closed-loop to open-loop gain. In a two-stage design (fig. 1b) each stage first produces open-loop intermodulation distortion (V_{e1}, V_{e2}) determined by the magnitude of the stage output signals (V_{out1}, V_{out2}) and third-order intercepts $(V_{OIP3,1}, V_{OIP3,2})$ through the relationships $V_{e2} = V_{out2}^3/V_{OIP3,2}^2$ and $V_{e1} = V_{out1}^3/V_{OIP3,1}^2 = (V_{out}/A_{V,2})^3/V_{OIP3,1}^2$. The closed-loop output is then $V_{out} = A_{CL}V_{in} + (A_{CL}/A_1)V_{e1} + (A_{CL}/A_1A_2)V_{e2}$. The amplifier must be frequency compensated for stability, $A_1A_2H = f_{unity}/jf$, by making either A_1 or A_2 vary at $1/jf$. In the first case if $A_1 \propto 1/jf$, the closed-loop distortion terms $(A_{CL}/A_1)V_{e1}$ and $(A_{CL}/A_1A_2)V_{e2}$ increase at high frequencies. In the second case if $A_2 \propto 1/jf$ for constant V_{out2}, V_{out1} varies as jf and V_{e1} consequently varies as $(jf)^3$ [6]. Distortion in either case increases at high frequencies.

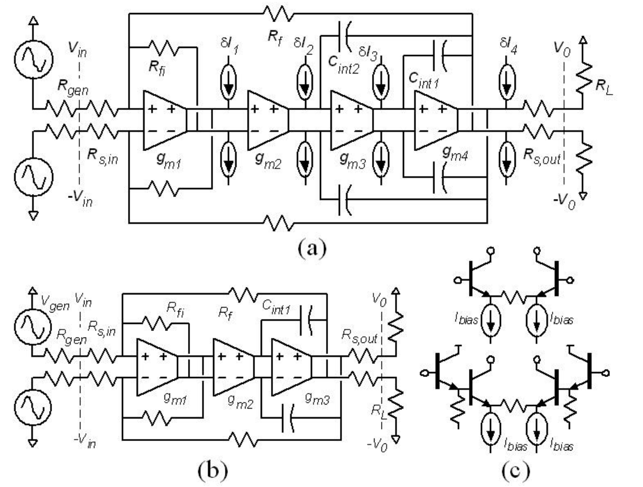

Fig. 2. Current-mode operational amplifiers in nested-Miller (a) and simple (b) form using HBT differential g_m blocks (c). Distortion currents are illustrated for the nested-Miller amplifier.

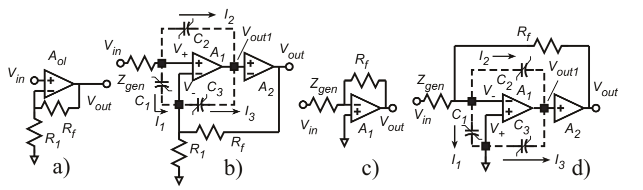

Fig. 3. Distortion from some non-linear impedances is not reduced by feedback. An elementary voltage-sum amplifier (a), when loaded by the non-linear input-stage capacitances (b) suffers from non-linear loading of the feedback network. An elementary current-sum amplifier (c), if constructed in multi-stage form (d) avoids these effects.

The amplifiers in this work are in current-mode form and use nested-(fig. 2a) or simple-(fig. 2b) Miller compensation. The blocks g_{mi} are degenerated HBT differential pairs (fig. 2c); the output stage (g_{m4} of fig. 2a, g_{m3} of fig. 2b) is a differential pair having emitter-follower input buffers. The nested-Miller amplifier (fig. 2a) consists of inner (g_{m3}, g_{m4}) and outer (g_{m2}, g_{m3}, g_{m4}) Miller integrators, and a transimpedance input stage (g_{m1}).

We now extend the earlier distortion analysis. Assume that $R_{s,out} << R_L$. With a two-tone ($f_1 = f_s + \varepsilon, f_2 = f_s - \varepsilon$) output signal, where each tone is of root-mean-square (RMS) amplitude V_{out}, the RMS currents of $(g_{m1}, ..., g_{m4})$ at f_1 and at f_2 are $I_{out4} \cong (1/R_L + j2\pi f_s(C_{int1} + C_{int2}))V_{out}$, $I_{out3} \cong j2\pi f_s C_{int1} V_{out}$, $I_{out2} \cong j2\pi f_s C_{int2} V_{out}$, and $I_{out1} \cong j2\pi f_s (C_{int2}/g_{m2}R_{fi})V_{out}$. Because of the $I_c = I_s \exp(qV_{be}/\eta kT)$ HBT characteristics, each stage produces distortion currents $(\delta I_1, ..., \delta I_4)$ at $(2f_1 - f_2, 2f_2 - f_1)$ of RMS amplitudes $\delta I_1 = I_{out1}^3/I_{OIP3,1}^2$, $\delta I_2 = I_{out2}^3/I_{OIP3,2}^2$, $\delta I_3 = I_{out3}^3/I_{OIP3,3}^2$, and $\delta I_4 = I_{out4}^3/I_{OIP3,4}^2$ – where each stage's output-referred IP3 is simply its DC bias current. The amplifier closed-loop gain is $A_{CL} = V_{out}/V_{gen} = R_f/(R_{gen} + R_{s,in})$, while $S_{21} \cong 2R_f/(Z_o + R_{s,in})$. The closed-loop output voltage contains frequency components at $(2f_1 - f_2, 2f_2 - f_1)$, each of RMS amplitude δV_{out}, where

$$\begin{aligned}\delta V_{out} = &\left(\frac{\delta I_4}{g_{m4}}\right)\left(\frac{jf}{f_{unity3-4}}\right)\left(\frac{jf}{f_{unity1-2-3-4}}\right)\\ &+\left(\frac{\delta I_3}{g_{m3}}\right)\left(\frac{jf}{f_{unity1-2-3-4}}\right)+\left(\frac{\delta I_2}{g_{m2}}\right)\left(\frac{R_f}{R_{fi}}\right)\\ &+\left(\frac{\delta I_1}{g_{m1}}\right)\left(\frac{R_f}{R_{s,in}+R_{gen}}+\frac{R_f}{R_{fi}}\right)\end{aligned} \quad (1)$$

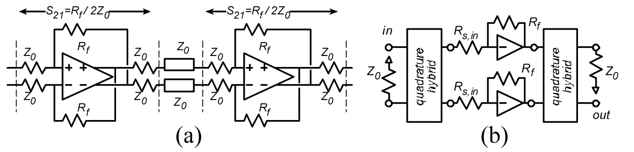

Fig. 4. Managing input and output impedances by (a) transmission-line series termination and (b) through the balanced amplifier configuration.

where $f_{unity3-4} = g_{m3}/2\pi C_{int1}$ is the unity-gain frequency of the inner Miller integrator and $f_{unity1-2-3-4} \cong (g_{m2}R_{fi}/C_{int2}R_f)$ is the unity-gain frequency of the feedback loop transmission, where $T \sim f_{unity1-2-3-4}/jf$. In a 350 GHz f_τ, f_{max} HBT technology, $f_{unity3-4} \sim$ 50-75 GHz and $f_{unity1-2-3-4} \sim$ 25-40 GHz are feasible. At $f_s \sim 2$ GHz, considerable reduction in the output stage distortion is therefore feasible. Compensation strongly impacts distortion, as the 2^{nd}-stage output current is $I_{out2} \cong j2\pi f_s C_{int2} V_{out}$ and becomes large at high frequencies. Analysis for the simple-Miller-compensated amplifier (fig. 2b) is similar, and correlates well with computer simulation and with experimental data.

Space prevents us from here addressing the general effects of non-linearities associated with the HBT junction capacitances C_{cb} and C_{je}. The effect of non-linear capacitive loading of the feedback network is however of paramount importance. In a simple series-shunt feedback amp (fig. 3a), low distortion is not obtained even with strong feedback. Considering separately (fig. 3b) the effect of the input (A_1) and subsequent (A_2) stages, in the limit of large loop gain $T = A_1A_2R_1/(R_f + R_1) \to \infty$; the differential input signal $(V^+ - V^-)$ is driven to zero, driving to zero the current I_1 associated with the non-linear input capacitance C_1. The voltages $(V^+ - V_{out1})$ and $(V^- - V_{out1})$ are driven *not to zero* but to $V_{in}(1 - A_{CL}/A_2)$ as $T \to \infty$; hence the currents (I_1, I_2) flowing through the input stage's non-linear base-collector capacitances (C_2, C_3) also remain nonzero. These currents (I_1, I_2) produce voltage drops across the feedback network impedances (Z_{gen}, R_1, R_f), producing closed-loop distortion even in the limit $T \to \infty$. The shunt-shunt feedback amplifier (fig. 3c,d) avoids this limitation – in the limit $A_2 \to \infty$, the voltages $(V^+ - V^-)$, $(V^+ - V_{out1})$, and $(V^- - V_{out1})$ are all driven to zero, forcing $(I_1, I_2, I_3) \to 0$. Our designs therefore use the shunt-shunt configuration.

The generator and load impedances will change the loop transmission T; unfavorable values may cause oscillation. We must clearly distinguish between stability in a 50 Ω system and stability with arbitrary generator and load (unconditional stability) impedance. Even before applying global feedback, the *open-loop* output impedance is low because of the local feedback through (C_1, C_2); hence even $\sim$5-10 Ω series padding $R_{s,out}$ provides a large range of *load* impedances for which the loop is stable. The transimpedance input stage (g_{m1}) provides an *open-loop* input impedance $R_{in,open-loop} \cong 1/g_{m1}$; provided that $||Z_{gen} + R_{s,in}|| < 1/g_{m1}$, T is then only weakly dependent upon Z_{gen}. This provides a wide range of *generator* impedances for which the loop is stable. Additionally, because the loop bandwidth is $\sim$20-50 GHz while $f_s \sim 2$ GHz, unconditional stability can be obtained by isolating at high frequencies the feedback amplifier from the external load using frequency-selective networks – as is standard in audio power amplifiers.

Finally, note that the shunt-shunt feedback forces $Z_{in} \to R_{s,in}$ and $Z_{out} \to 0\ \Omega$. If impaired noise figure and output power can be accepted, matched line interfaces can be provided by series padding (fig. 4a). For highest OIP3 and lowest noise figure, one must set $R_{s,in} << Z_o$ and $R_{s,out} << Z_o$, which leads to poor S_{11} and S_{22}. In this case, a balanced amplifier configuration (fig. 4b) will provide low return losses over an octave of bandwidth even with minimal or zero series input and output padding.

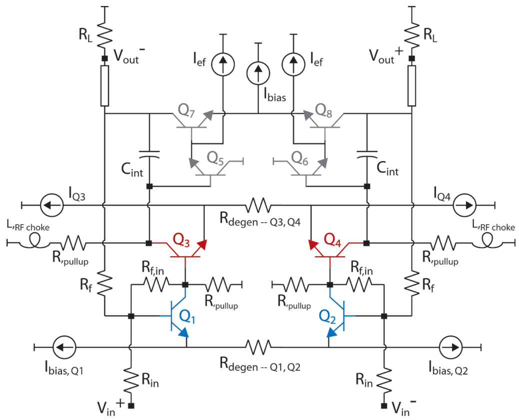

Fig. 5. Circuit diagram of the simple-Miller-compensated op-amp.

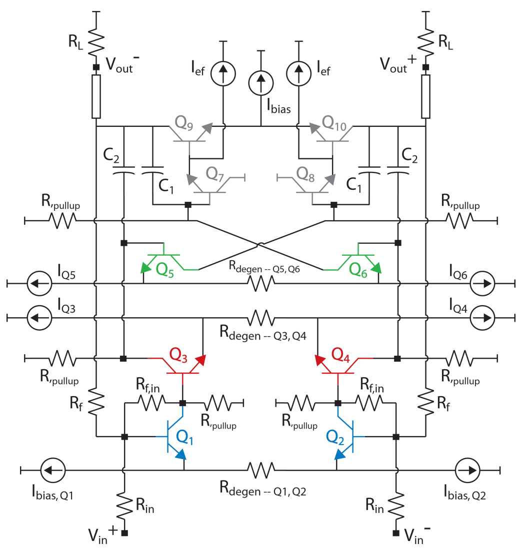

Fig. 6. Circuit diagram of the nested-Miller-compensated op-amp.

III. Design

A simple resistive feedback network is used for these circuits. To ensure the network remains dominantly real across the 3dB bandwidth of the op-amp, the length of the feedback path ($Z_o = 50\ \Omega$) is only 70 μm (simple-compensation) or 90 μm long (nested-compensation) in order to avoid series inductance or shunt capacitance loading on the interconnect. Such a short length is possible with the symmetric, folded scheme used for circuit layout, shown in schematic form in figures 5 and 6. For both amplifiers R_f = 300 Ω, R_{in} = 50 Ω, and $R_{f,in}$ = 250 Ω.

For the simple-Miller compensated op-amp (fig. 2b, 5), the bias currents are set through the use of pulldown resistors and the bias voltage at the base for a given amplifier stage is set by the potential drop $I_{Q,i}R_{pullup,i}$ of the preceeding stage (as *pnp* HBTs are not available). Because the bias current of stage-2 is large, $R_{pulldown,2}$ must be small to appropriately set the voltage for stage-3. In order to avoid the large distortion that would come from only having $R_{pullup,2}$ loading the collector of stage-2, a large 6 nH inductor is placed in-series to act as an RF choke where $Z = R_{pullup,2} + j\omega L$, increasing the impedance from 50 to 125 Ω. To improve the output return-loss and amplifier stability, 7.5 Ω of series padding is added at the output. Amplifier stability is also improved through the use of a shunt 500 fF capacitor set in the middle of the input resistor forming an RCR (5Ω-500fF-45Ω) damping filter – permitting higher loop bandwidths to be pursued for increased distortion suppression at the expense of lower overall amplifier bandwidth.

TABLE I

Detailed bias conditions for the simple-Miller compensated op-amp from fig. 5. C_{int} is varied from 250fF down to 125fF.

V_{ee}=-4.6V	stage 1	stage 2	stage 3,EF	stage 3,diff
g_m (mS)	45	61, 70, 95	N/A	547
$I_{Q\ x,y}$ (mA)	10	30	14	56
P_{DC} (mW)	92	276	129	515

TABLE II

Detailed bias conditions for the nested-Miller compensated op-amp from fig. 6.

V_{ee}=-4.6V	stage 1	stage 2	stage 3	stg 4,EF	stg 4,diff
g_m (mS)	40	46	56	N/A	455
$I_{Q\ x,y}$ (mA)	11	30	15	15	36
P_{DC} (mW)	101	276	138	138	331

For the nested-Miller compensated op-amp (fig. 2a, 6), the bias currents are set in the same manner as its simple-compensated counterpart. These designs employ 7.5 Ω of series output padding as well, but do not utilize an input dampening filter. The nested-amp reported here does not utilize RF choke inductors in series with the low impedance pullup resistors – this facilitates significant distortion generation at the HBT collector node of the respective stages, making OIP3 poor. While nested-compensated amps were designed, simulated, and fabricated using RF choke inductors, measured results revealed severe amplifier instability and oscillation – efforts are ongoing to better understand this inconsistency.

Figure 7 shows an IC micrograph of a simple-compensated op-amp. Details of the InP HBT process from Teledyne Scientific have been reported [3], where inverted, thin-film dielectric (Benzocyclobutene, 3 μm thick) microstrip wiring is employed and the top-most metal layer is used as the ground plane. Both amplifiers are biased by a single voltage source -4.6 V_{ee}, and voltage offsets $V_{in} \cong$ -2.15V and $V_{out} \cong$ -460mV are required. Tables I (simple-compensation) and II (nested-compensation) summarize the biasing (I_Q and P_{DC}) and g_m of the various stages in the amplifiers.

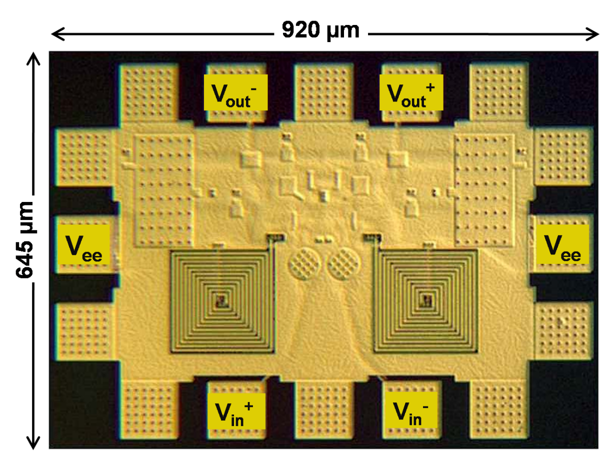

Fig. 7. IC micrograph of the simple-Miller compensated op-amp.

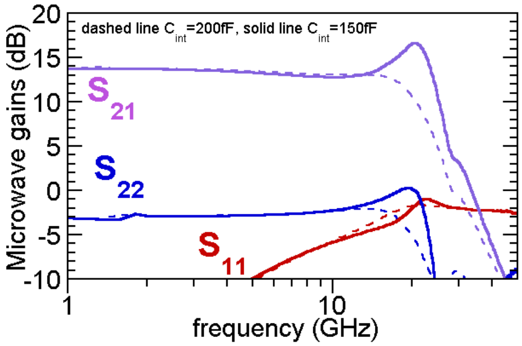

Fig. 8. Measured differential S-parameters of the simple-Miller compensated op-amps.

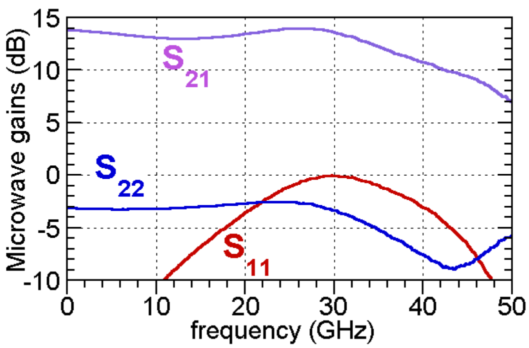

Fig. 9. Measured differential S-parameters of the nested-Miller compensated op-amp.

IV. Measurement Setup

4-port RF measurements of the circuits were performed using a 10MHz-50GHz (Agilent E8364B, N4421B) network analyzer after SOLT calibration.

For two-tone power and IM3 measurements, the test-bench here employs two synthesizers operating at 1.950 and 1.975 GHz. Their respective outputs pass through 6dB of attenuation, a low-pass filter, and two 20dB isolators before being brought together by a power combiner. A differential two-tone signal is created by way of a 180° hybrid-ring and applied on-wafer. The differential output is combined and measured. Output loss associated with the cabling and hybrid-ring between the probes and spectrum analyzer was measured by 3-port S-parameters and is 5.0 dB. Measurement of a differential thru-line shows 55-56 dBm OIP3 of residual system distortion. This permits IM3 measurements of amplifiers having OIP3 $<$ 52 dBm.

V. Op-Amp Circuit Results

Figure 8 shows the microwave gains for two single-Miller compensated op-amps, where they are identical except one employs 200 fF C_{int} and the other 150 fF C_{int} – already discussed. The nominal S_{21} gain is 13.8dB and P_{DC} = 1013 mW. For the op-amp employing 200 fF C_{int}, the 3dB bandwidth is 19.8 GHz, with 0.7dB of gain droop and no peaking. For the op-amp employing 150 fF C_{int}, the 3dB bandwidth is 24.8 GHz, with 1.0dB of gain droop and 2.8dB of peaking. From the Rollett stability factor K, 200 fF of compensation is just enough to permit unconditional amplifier stability across the 50 GHz measurement span. This is not the case for the op-amp employing 150 fF C_{int} – it is only unconditionally stable from DC to 15.0 GHz, while conditionally stable in a 50 Ω system across the 50 GHz measurement span.

Figure 9 shows the microwave gains for the nested-Miller compensated op-amp. The nominal S_{21} gain is 13.8dB with gain ripple less than ± 0.8 dB, and the 3dB bandwidth is 40 GHz – where C_{int1} = 100 fF and C_{int2} = 125 fF. P_{DC} = 993 mW. From the Rollett stability factor K, the amplifier is unconditionally stable from DC-20 GHz and conditionally stable in a 50 Ω system across the 50 GHz measurement span.

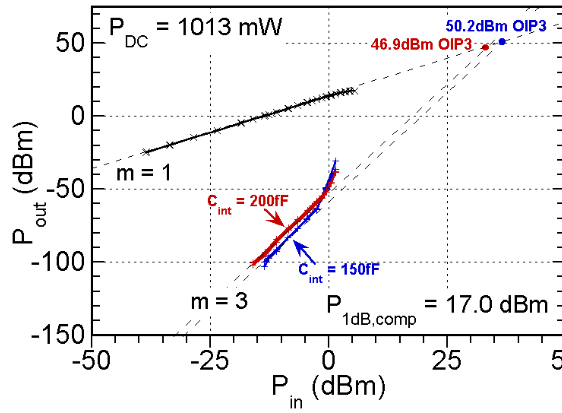

Fig. 10. Two-tone power and IM3 measurements for the simple-Miller compensated op-amps whose RF data is shown in fig. 8.

Differential two-tone power measurements ($f_{1,2}$ = 1.950, 1.975 GHz) for the simple-Miller compensated op-amps are shown in figure 10. The expected P_{in} versus P_{out} trends for the fundamentals and IM3 products (f_{IM3} = 1.925, 2.000 GHz) are clearly observed, and the intercept superimposed on the graph agrees very well with the OIP3 calculation from discrete values of P_{in}, where

$$OIP3(dBm) = P_{out,fund} + \frac{P_{out,fund} - P_{IM3}}{2} \quad (2)$$

For the op-amp with 200 fF C_{int}, the IM3 measurements show the OIP3 is 46.9 dBm – where its OIP3 to P_{DC} ratio is 49. For the op-amp with 150 fF C_{int}, the OIP3 is 50.2 dBm – where its OIP3 to P_{DC} ratio is 103. The results here represent a 1.5 and 3.2× betterment in state-of-the-art [5] at a similar operating frequency. As the two-tone output power approaches 11.5 dBm, higher order IM_X distortion dominates as the output stage HBTs are beginning to operate into quasi-saturation (Kirk-effect, non-linear C_{cb}). The P_{1dB} compression is 17.0 dBm.

While not shown, similar two-tone measurements were performed on the nested-Miller compensated op-amp, where the OIP3 is only 42.8 dBm (OIP3/P_{DC} = 19.2). The dominant distortion is associated with the use of only small pull-up resistors, which has already been discussed in the design section of this paper. As the two-tone output power approaches 9 dBm, higher order IM_X distortion dominates the measurement. The P_{1dB} compression is 13.7 dBm.

Acknowledgment

This work was supported by the DARPA FLARE program. Special thanks to Program Managers Dr. Steve Pappert and Dr. Sanjay Raman, and Dr. Richard Eden for their contributions and support.

References

[1] J.E. Solomon *et al.*, *IEEE Journal of Solid-State Circuits*, Vol. SC-9, No. 6. Also at http://www.national.com/an/AN/AN-A.pdf
[2] M.J.W. Rodwell *et al.*, *Journal of Solid-State Circuits*, Vol. 26, No. 10, pp. 1378-1382, October 1991.
[3] M. Urteaga *et al.*, *Proc. Device Research Conference*, Notre Dame, IN, pp. 239-240, June 21-23, 2004.
[4] S.P. Voinigescu *et al.*, *Proc. IEEE Compound Semiconductor Integrated Circuits Symposium*, pp. 283-286, Nov. 2005.
[5] WJ Communications website – http://www.wj.com/products/productviewform.aspx?productsku=AS103A
[6] E. Cherry, *IEEE Transactions on Acoustics, Speech, and Signal Process*, Vol. 29, Iss. 2, Apr. 1981, pp. 137-146.